VIBRO-VISUAL IMAGE FEATURE EXTRACTION WITH CORRELATION IMAGE SENSOR

Circular and Doubly Circular Vibration for Arbitrary Complex Differentials

Shigeru Ando and Toru Kurihara

Department of Information Physics and Computing, University of Tokyo, Tokyo, Japan

Keywords: Optical Flow Equation, Weighted Integral Method, Modulated Imaging, Correlation Image Sensor, Computer Vision, Velocity Field Measurement, Particle Image Velocimetry.

Abstract: In VISAPP 2009, we showed that exact optical flow can be determined using only a single pixel and frame of the correlation image sensor(Ando et al., 2009). In this paper, using the newest device of it, we present a theory and experimental evaluation of a bio-inspired vibro-visual correlation imager with various feature extraction capability. Mimicking the involuntary movement (microsaccade) of human eyes, it vibrates rapidly and finely a mirror in its visual axis so as to generate an equivalent vibration of every pixel in a doubly circular locus. The time-varying intensity is captured by a correlation image sensor (CIS) with synchronous reference signals to the vibration, and complex first/second order differentials and Laplacian are obtained as the image features. General theoretical foundations and an implementation result of this system using a novel 640×512 pixel device are presented. Several experimental results using it including a realtime control of resolution and edge detection from a combined use of the first and second order differentials are shown.

1 INTRODUCTION

For image recognition systems, tasks for extracting brightness gradient, edges, corners, ridges, etc. and localizing them accurately are extremely important. Almost all methods proposed so far are for an image array that has captured already by a sensing device. In those methods, reduction of various noises and artifacts caused by the sensing device and spatio-temporal integration/sampling through it has been treated as one of major subjects for achieving a satisfactory performance (Ando, 2000b; Ando, 2000a). The spatio-temporal sampling/quantization before extracting those structures by conventional image sensors is often a significant obstacle to perform desired, detailed, and accurate analysis of them.

The goal of our study is the realization of vibro-visual imaging system mimicking involuntary eye movements of human vision that can extract important image features during the capturing process of continuous intensity distribution (Ando et al., 2002; Hontani et al., 1999; Hontani et al., 2002). The involuntary eye movements are the small and perpetual vibration of eyeball when the human vision gazes at an object. When the image sensor is vibrated in a period sufficiently shorter than the frame interval, the continuous intensity distribution on its surface is counter-vibratorily shifted. This causes a time-varying incident light, i.e., temporal modulation, on the pixel according to the local structure of the intensity distribution around the pixel. The temporal modulation based sensing scheme of spatial structures, being free from spatio-temporal sampling/quantization error, have been studied in various areas (Tang, 1978; Ikuta, 1985; Storrs and Mehrl, 1994; Hlyo and Samms, 1986; Wang et al., 1997; Hongler et al., 2003), but most of them are for point-by-point sensing. Our study is different in the use of parallel imaging/demodulation device, i.e., the correlation image sensor (Ando and Kimachi, 2003; Ando et al., 2007; Han et al., 2010) for this purpose. In this paper, we present theoretical foundation and experimental evaluation of a bio-inspired vibro-visual correlation imager with various feature extraction capability. Novel doubly circular vibration and simultaneous three frequency demodulation schemes are introduced. Theoretical foundation is constructed by using complex differential (d-bar) operator theory.

Ando S. and Kurihara T..
VIBRO-VISUAL IMAGE FEATURE EXTRACTION WITH CORRELATION IMAGE SENSOR - Circular and Doubly Circular Vibration for Arbitrary Complex Differentials.
DOI: 10.5220/0003838701860191
In *Proceedings of the International Conference on Computer Vision Theory and Applications* (VISAPP-2012), pages 186-191
ISBN: 978-989-8565-03-7

2 THEORY

2.1 Complex Differential Operator

Let us introduce a coordinate transform

$$(x,y) \to (z,z^*) = (x+jy, x-jy) \tag{1}$$

in the image plane (x,y) (j: imaginary unit). Any function f of (x,y) can be expressed equivalently using the coordinate (z,z^*) as $f(z,z^*)$. The differentials in (z,z^*) are also expressed as(Brandwood, 1983; van den Bos, 1994)

$$\frac{\partial}{\partial z^*} \equiv \frac{1}{2}(\frac{\partial}{\partial x} + j\frac{\partial}{\partial y}), \quad \frac{\partial}{\partial z} \equiv \frac{1}{2}(\frac{\partial}{\partial x} - j\frac{\partial}{\partial y}). \tag{2}$$

For simplicity of notation, we often abbreviate the coefficient $1/2$. The first order complex differentials are the complex notation of gradient vector and its conjugate as

$$\frac{\partial f}{\partial z^*} = \frac{\partial f}{\partial x} + j\frac{\partial f}{\partial y}, \quad \frac{\partial f}{\partial z} = \frac{\partial f}{\partial x} - j\frac{\partial f}{\partial y},$$

and the second order ones are the complex second order differential and Laplacian as

$$\begin{aligned} \frac{\partial^2 f}{\partial (z^*)^2} &= \frac{\partial^2 f}{\partial x^2} - \frac{\partial^2 f}{\partial y^2} + 2j\frac{\partial^2 f}{\partial x \partial y} \\ \frac{\partial^2 f}{\partial z \partial z^*} &= \frac{\partial^2 f}{\partial x^2} + \frac{\partial^2 f}{\partial y^2}. \end{aligned}$$

All of them are greatly important as primitive image features for image pattern recognition and understanding.

By using the complex differentials, the Taylor expansion of $f(\zeta,\zeta^*)$ around $(0,0)$ is expressed as

$$\begin{aligned} f(\zeta,\zeta^*) &= \sum_{r=0}^{\infty} \frac{1}{r!} (\zeta\frac{\partial}{\partial z} + \zeta^*\frac{\partial}{\partial z^*})^r f(0,0) \\ &= \sum_{r=0}^{\infty} \frac{1}{r!} \sum_{k=0}^{r} \left(\begin{array}{c} r \\ k \end{array} \right) \zeta^k (\zeta^*)^{r-k} \frac{\partial^r f(0,0)}{\partial z^k \partial (z^*)^{r-k}}. \end{aligned} \tag{3}$$

2.2 Circular Vibratory Scan

Let us consider first a circular vibratory scan with radius ε ($\sim$ a few pixels long) and angular velocity ω. Let us place the origin at a pixel of interest. Then, using the Taylor expansion formula for complex differentials, the time-varying intensity received by the pixel is expressed as

$$\begin{aligned} f(t) &= f(\varepsilon e^{j\omega t}, \varepsilon e^{-j\omega t}) \\ &= \sum_{r=0}^{\infty} \frac{\varepsilon^r}{r!} \sum_{k=0}^{r} \left(\begin{array}{c} r \\ k \end{array} \right) e^{j(2k-r)\omega t} \frac{\partial^r f(0,0)}{\partial z^k \partial (z^*)^{r-k}}, \end{aligned} \tag{4}$$

in which $e^{j(2k-r)\omega t}$ is the time-varying term corresponding to the $(2k-r)$th harmonic component of the circular rotational frequency ω. The other terms involving the complex rth order differential $\partial^r f(0,0)/\partial z^k \partial (z^*)^{r-k}$ is the amplitude of this harmonic component.

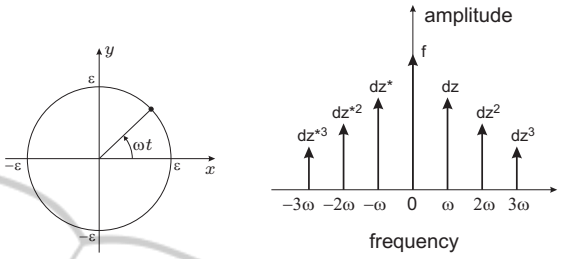

(a) circular vibration (b) frequency components

Figure 1: Circular vibratory scan and its spectral encoding of complex differentials. The dz and dz* in (b) indicate $\partial/\partial z$ and $\partial/\partial z^*$, respectively.

To understand the meaning of summation on r and k, let us illustrate visually the terms taking $2k-r$ (order of harmonics) as horizontal axis and r (order of amplitude ε) as vertical axis. They are then expressed as

	−4	−3	−2	−1	0	1	2	3	4
1					1				
1				ε		ε			
1/2			ε²		2ε²		ε²		
1/6		ε³		3ε³		3ε³		ε³	
1/24	ε⁴		4ε⁴		6ε⁴		4ε⁴		ε⁴

Namely, for example, the $2k-r=0$ frequency component (DC) locating at the center is constructed by a sum of 1, $\partial^2 f(0,0)/\partial z \partial (z^*)$, $\partial^4 f(0,0)/\partial z^2 \partial (z^*)^2, \cdots$ complex differentials with each amplitude $1, (1/2)\times 2\varepsilon^2, (1/24)\times 6\varepsilon^4, \cdots$, respectively. For the $2k-r=1$ frequency component (ω), it is constructed by $\partial f(0,0)/\partial z$, $\partial^3 f(0,0)/\partial z^2 \partial z^*, \cdots$. Here, let us assume the radius ε of circular vibration is sufficiently small and the intensity distribution $f(z,z^*)$ is sufficiently smooth. Then, the lowest order term of ε in each frequency component can be expected to be sufficiently larger than the higher order terms. This means the lowest order term dominates in each frequency component individually, and hence, the time-varying intensity is expressed as

$$f(t) \simeq \sum_{r=0}^{\infty} \frac{\varepsilon^r}{r!} (\frac{\partial^r f(0,0)}{\partial z^r} e^{jr\omega t} + \frac{\partial^r f(0,0)}{\partial (z^*)^r} e^{-jr\omega t}) \tag{5}$$

(notice this expression is valid only under usage after frequency decomposition). This shows that the amplitude and phase of frequency component of $r\omega$ is just

equal to rth order complex differential. For positive frequency components, we can obtain the complex differential of the same order as the complex amplitude of the harmonics. For negative frequency components, we can obtain the conjugate complex differential.

A significant drawback of this vibrating scheme is that complex differentials composed of both $\partial/\partial z$ and $\partial/\partial z^*$ such as Laplacian can not be obtained as the dominant term of frequency component. A solution to this problem will be given in the next section.

2.3 Doubly Circular Vibratory Scan

As an extension, the doubly circular vibration is the scan shown in Fig. 2(a) along the locus

$$(z, z^*) = (\mathcal{E} e^{j\Omega t} + \varepsilon e^{j\omega t}, \mathcal{E} e^{-j\Omega t} + \varepsilon e^{-j\omega t})$$

where $\Omega \ll \omega$ and the radii ε and $\mathcal{E}$ are both small enough. Therefore the Taylor expansion is expressed as

$$\begin{aligned} f(t) = & \sum_{r=0}^{\infty} \frac{1}{r!} \sum_{k=0}^{r} \binom{r}{k} \\ & \times (\mathcal{E} e^{j\Omega t} + \varepsilon e^{j\omega t})^k (\mathcal{E} e^{-j\Omega t} + \varepsilon e^{-j\omega t})^{r-k} \\ & \times \frac{\partial^r}{\partial z^k \partial (z^*)^{r-k}} f(0,0). \end{aligned}$$

Using a similar argument as in the previous section, we obtain an expression of the time-varying intensity as

$$\begin{aligned} f(t) \simeq & \sum_{r=0}^{\infty} \sum_{s=0}^{\infty} \frac{\varepsilon^r}{r!} \frac{\mathcal{E}^s}{s!} \{ e^{j(r\omega + s\Omega)t} \frac{\partial^{r+s}}{\partial z^{r+s}} f(0,0) \\ & + e^{j(r\omega - s\Omega)t} \frac{\partial^{r+s}}{\partial z^r \partial (z^*)^s} f(0,0) \\ & + e^{j(-r\omega + s\Omega)t} \frac{\partial^{r+s}}{\partial (z^*)^r \partial z^s} f(0,0) \\ & + e^{j(-r\omega - s\Omega)t} \frac{\partial^{r+s}}{\partial (z^*)^{r+s}} f(0,0) \}, \end{aligned} \quad (6)$$

which shows that the amplitude and phase of frequency component of $r\omega + s\Omega$ is just equal to the complex differential $\partial^{r+s} f / \partial u^r \partial v^s$ where $u, v \equiv z$ when $r, s > 0$ and $u, v \equiv z^*$ when $r, s < 0$. The spectral distribution is shown in Fig. 2(b).

3 SYSTEM AND EXPERIMENTS

3.1 Optical Setup

The photographs of the setup are shown in Figs. 3 (a) and (b). The doubly circular vibration of optical

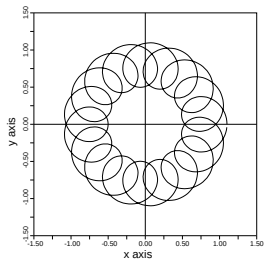

(a) locus of a doubly circular scan

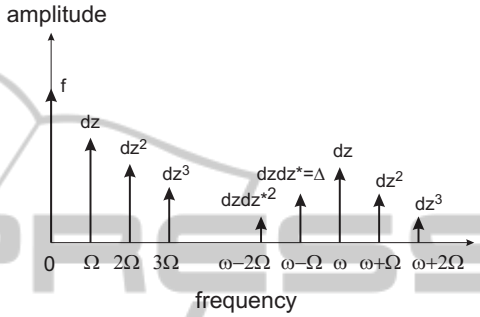

(b) frequency components

Figure 2: Doubly circular vibratory scan and its spectral encoding of complex differentials. (a) $\varepsilon = 0.3$, $\mathcal{E} = 0.8$, and $\omega/\Omega = 18$, (b) spectral components, dz and dz* indicate $\partial/\partial z$ and $\partial/\partial z^*$, respectively.

axis was given by a 2-D angularly oscillating mirror driven directly synchronously by the camera. It is inserted in front of the imaging lens in 45 deg angle to capture the object in 90 deg angle from the camera. The frame frequency was chosen as 12Hz to avoid an interference with ambient light frequencies (50Hz and 100Hz). The driving signals are a mixture of sinusoidal waves with frequencies $\Omega/2\pi = 12$Hz and $\omega/2\pi = 48$Hz. The amplitudes of them can be changed freely during the capturing operation by changing the volume control of audio-amplifiers used to drive the oscillating mirror.

3.2 Experimental Results

a) Extraction of Complex 1st and 2nd Differentials Examples of the results are shown in Figs.4 (a), (b), and (c). Three images display the intensity, complex gradient, and complex 2nd-order differential fields of a moving doll. The phase of the complex image is shown by the hue of color image. In (a), the doubly circular vibration locus is captured in a specularly highlighted part. The complex 1st order differential is equivalent to the gradient vector. So, it can be used to extract edges or to analyze orientational features of texture. The complex 2nd order differential shows zero-cross lines at edges and the phase (double of the edge angle) is inverted across the line. Therefore, it

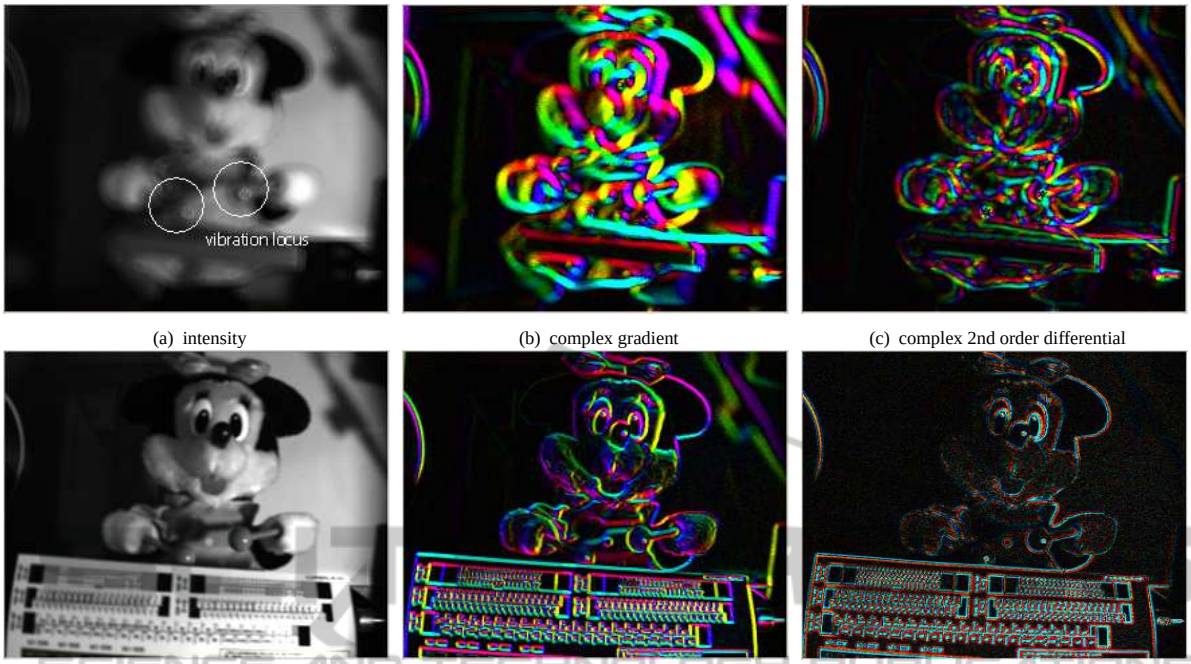

(a) intensity (b) complex gradient (c) complex 2nd order differential

(d) intensity (e) complex gradient (f) Laplacian

Figure 4: Example of experimental results. (a) and (d) show the intensity images, (b) and (c), respectively, show the complex first and second differential image for (a), and (f) shows the Laplacian image for (a). The phase in $[0, 2\pi]$ is represented by colors from red to violet.

(a) setup (b) CIS and vibrating mirror

Figure 3: Photographs of the experimental setup and vibrating mirror. The vibration is given by the 2-axis angularly vibrating mirror between the object and the camera. The frame frequency is 12Hz, the vibration frequencies are $\Omega/2\pi = 12$Hz and $\omega/2\pi = 48$Hz.

can be used to extract and localize edges accurately.

b) Extraction of Complex 1st Differential and Laplacian

Examples of the results are shown in Figs.4 (d), (e), and (f). In (e), strength and orientation of edges and ridges of a resolution chart are displayed. (f) shows the Laplacian. It is displayed in only two hues corresponding to opposite signs because the Laplacian for an real-valued image is always real. The amplitude of Laplacian becomes higher where the brightness curvature is large such as rising and falling lines of edges or top of ridges. Those features are captured significantly clearly.

c) Vibration Amplitude vs. Feature Response

Fig. 5 (a) to (d) show the result. When the vibration amplitude is very small as shown in (a), the image captures very detailed features smaller than the pixel interval. According to the increase of the vibration amplitude from (a) to (c), the captured images tend to respond to smoothed low frequency features more and more. This property is desirable for the realtime adaptive processing of image scenes. In (d), the vibration amplitude is maximized. Although detailed features are eliminated, image captures with very high signal-to-noise ratio the overall orientational features, e.g., edges and/or textures, of object and background.

d) Application to Edge Detection

Figs. 6 (a) and (b) show an example of edge detection from complex differentials. Two set of reference signals with frequencies $\Omega/2\pi = 12$Hz and $\Omega/\pi = 24$Hz were supplied. (a) shows the intensity image. Its blur is caused by the doubly circular vibration. (b) shows the edge image extracted from the zero-cross of the complex 2nd order differential. The color indicates the edge orientation determined by the phase of complex gradient image captured simultaneously.

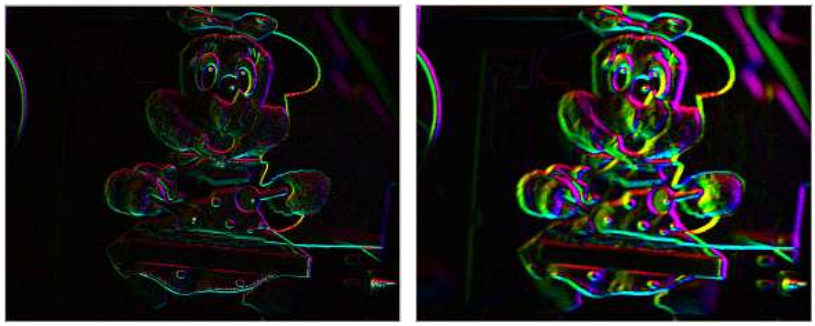

(a) low vibration amplitude (b) middle vibration amplitude

(c) high vibration amplitude (d) maximum vibration amplitude

Figure 5: Complex gradient images under gradually increasing level of vibration amplitude. In (a), features smaller than the pixel interval are extracted. The phase in $[0, 2\pi]$ is represented by a color from red to violet.

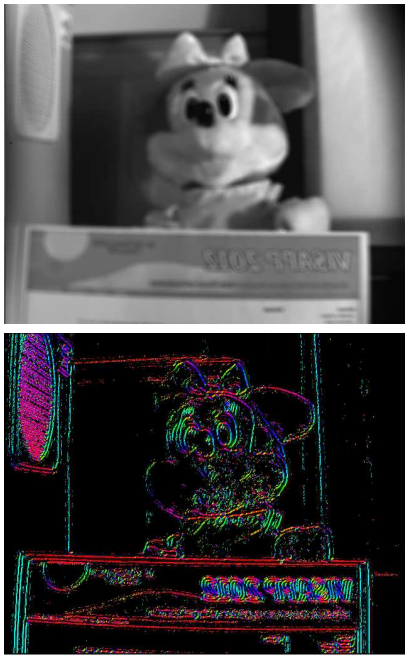

(a)

(b)

Figure 6: Example of edge detection from complex differentials. (a) and (b), respectively, show the intensity image and the edge image extracted from the zero-cross of the complex 2nd order differential. The color indicates the edge orientation.

4 CONCLUSIONS

Theoretical foundation and experimental evaluation of a bio-inspired vibro-visual correlation imager were presented. Implementation and several experimental results of this system using a novel 640×512 pixel device are presented including an application to edge detection. Although the performance of correlation image sensor are in a depeloping level, the sensitivity and accuracy of image features captured by it were exceptionally good. Therefore, we consider the proposed vibro-visual imaging system is sufficiently promising for future applications.

REFERENCES

Ando, S. (2000a). Consistent gradient operators. In *IEEE Trans. PAMI, vol.22, no.3, pp.252-265*.

Ando, S. (2000b). Image field categorization and edge/corner detection from gradient covariance. In *IEEE Trans. PAMI, vol.22, no.2, pp.179-190*.

Ando, S. and Kimachi, A. (2003). Correlation image sensor: Two-dimensional matched detection of amplitude modulated light. In *IEEE Trans. Electron Devices, vol.50, no.10, pp.2059-2066*.

Ando, S., Kurihara, T., and Wei, T. (2009). Exact algebraic

method of optical flow detection via modulated integral imaging - theoretical formulation and real-time implementation using correlation image sensor –. In *Proc. VISAPP 2009, pp.480-487, Lisboa*.

Ando, S., Nara, T., Ono, N., and Kurihara, T. (2007). Real-time orientation-sensitive magneto-optic imager for leakage flux inspection. In *IEEE Trans. Magnetics, vol.43, no.3, pp.1044-1051*.

Ando, S., Ono, N., and Kimachi, A. (2002). Involuntary eye-movement vision based on three-phase correlation image sensor. In *Proc. 19th Sensor Symp., pp.83-86, Kyoto*.

Brandwood, D. H. (1983). A complex gradient operator and its application in adaptive array theory. In *IEE Proc. vol.130, no.1, pp.11-16*.

Han, S., Sawada, T., Iwahori, T., Kawahito, S., and Ando, S. (2010). Three-phase time-correlation image sensor using pinned photodiode active pixels. In *IS&T/SPIE Electronic Imaging, 7536-28*.

Hlyo, N. and Samms, R. W. (1986). Combined optimization of image-gathering optics and image-processing algorithm for edge detection. In *J. Opt. Soc. Am., vol. 3, no. 9, pp.1522-1536*.

Hongler, M., de Meneses, Y. L., Beyeler, A., and Jacot, J. (2003). The resonant retina: exploiting vibration noise to optimally detect edges in an image. In *IEEE Trans. Pattern Anal. Machine Intell., vol.25, no.9, pp.1051-1062*.

Hontani, H., Kimachi, A., and Ando, S. (1999). Involuntary eye movement vision and its applications. In *Trans. IPSJ, CVIM, 118-2*.

Hontani, H., Shibata, J., Kimachi, A., and Ando, S. (2002). Vibratory image feature extraction based on local log-polar symmetry. In *Trans. IPJ, vol.43, no.7, pp.2309-2318*.

Ikuta, T. (1985). Active image processing. In *Applied Optics, vol. 24, no.18, pp.2907-2913*.

Storrs, M. and Mehrl, D. J. (1994). Detection of spatial derivatives of images using spatiotemporal techniques. In *Optical Engineering, vol. 33, no. 9, pp.3072-3081*.

Tang, C. L. (1978). Dithered-beam metrology. In *Applied Optics, vol.17, pp.3865-3868*.

van den Bos, A. (1994). Complex gradient and hessian. In *IEE Proc. Vis. Image Signal Process., vol.141, no.6, pp.380-382*.

Wang, C., Ni, Y., and Devos, F. (1997). A spatio-temporal differentiation light sensor. In *Sensor and Actuators A, vol. 62, pp.492-495*.